

Hominin home ranges and habitat variability: exploring modern African analogues using remote sensing

Authors: Hannah J. O'Regan¹, David M. Wilkinson², Christopher G. Marston³

¹ Department of Archaeology, School of Humanities, University of Nottingham, Nottingham, NG7 2RD, UK.

² School of Natural Sciences and Psychology, Liverpool John Moores University, Liverpool, L3 3AF, UK.

³ Department of Geography, Edge Hill University, Ormskirk, Lancashire, L39 4QP, UK

Abstract

The palaeoanthropological literature contains numerous examples of putative home range sizes associated with various hominin species. However, the resolution of the palaeoenvironmental record seldom allows the quantitative analysis of the effects of different range sizes on access to different habitat types and resources. Here we develop a novel approach of using remote sensing data of modern African vegetation as an analogue for past hominin habitats, and examine the effects of different range sizes on the access to habitat types. We show that when the location of the ranges are chosen randomly then the number of habitat types within a range is surprisingly scale invariant – that is increasing range size makes only a very modest difference to the number of habitat types within an estimated hominin home range. However, when transects are placed perpendicular to a water body (such as a lake or river bank) it is apparent that the greatest number of habitats are seen near water bodies, and decline with distance. This suggests additional advantages to living by freshwater other than the obvious one associated with access to drinking water, and may indicate that the finding of hominins in fluvial and lacustrine deposits is not simply a taphonomic issue.

Introduction

In the nineteenth and early twentieth century relatively little emphasis was given to the environmental context in studies of human evolution – this started to change in the 1930's around the time of the 'evolutionary synthesis' (Bowler, 1986). While there is now some consensus in the literature that many early hominins in Africa lived in mosaic habitats (see Reynolds et al. (2015) for a review and history of this terminology), little work has been undertaken on how variable habitats might have been within hominin home ranges. While site-level analyses can produce highly detailed results (e.g. Kroll and Isaac, 1984; Magill et al. 2016), and analyses integrating climate and palaeoproxies have been undertaken at a continental scale (e.g. Blome et al., 2012), very little detailed landscape reconstruction has been attempted at the level of individual hominins or their social groups. Here we take a novel approach to hominin spatial ecology by using remote sensing to quantify patterns in the vegetation of modern Africa at hominin-relevant scales, to examine the distribution and habitat variability that may have been encountered in the past. Such an approach has the obvious disadvantage of characterising the modern vegetation, rather than the vegetation at the time of interest for any given past hominin species. However, it does allow variation to be quantified at a far greater spatial and narrower temporal scale than is possible based on palaeoenvironmental proxies such as pollen, pedogenic carbonate analysis or phytoliths (although these can be incorporated, see below), or from traditional field-based approaches. We explore these advantages here, using data from seven separate regions of sub-Saharan Africa to quantify habitat variability at a variety of hominin-relevant scales.

We are particularly considering the range sizes and habitat variability associated with various species of *Australopithecus* and early *Homo*, although the methods are equally applicable to earlier and later hominin taxa. While it is obvious that hominins lived on and within the landscape, we have few tools at our disposal to examine exactly how different habitat types may have influenced their movements. Suggested key characteristics are the presence of water (Ashley et al. 2009; Finlayson, 2014; Quinn et al. 2013), trees for shade (Habermann et al., 2016), and river cobbles or outcrops for tool making (Harmand, 2009). It is rare, however, to have stone tools or cutmarked bones directly associated with palaeoenvironmental proxies that can be used to reconstruct that exact location (although FLK Zinj may be a notable exception, Magill et al. 2016). Rather than seeking to reconstruct a particular place at a specific point in time (which can usually only be achieved on a scale of tens to hundreds of metres, rather than the kilometres that hominins are likely to have ranged), we are examining vegetation at a larger scale to look for physical patterns – such as the number of different habitat types a hominin may have encountered in a daily round, or even within

their lifetime. If the presence of a number of different habitat types such as trees, bushes, water, swamp or bare rock was important to hominins, then we can examine how likely it is that such variability is would have been encountered on a regular basis or at specific locations (such as riversides) using vegetation classifications derived from modern remote sensing.

This new approach allows us to consider, for measures identified in the fossil record (e.g. % canopy cover, Cerling et al. 2011; Quinn et al., 2013) and vegetation patchiness (i.e. 'mosaic' habitats), how the land cover in modern Africa varies on a number of hominin-relevant scales. Questions such as 'how many vegetation types would typically be found within the putative range size of a given hominin species and how does this number vary as range size increases (or decreases)?'. In this paper we set out the basic ideas of this approach – which is intended to be complimentary to, rather than replacing, existing ways of addressing these questions. We use our data to address two specific points:

1) We look at randomly placed home ranges and calculate land cover within them. This allows us to quantify the effect of increasing range size on access to different vegetation types.

2) We focus on water, and examine how land cover and patchiness change as one moves away from water sources.

Note that we are not attempting to reconstruct past environments, rather quantifying the landscape as it is today (with adjustment for anthropogenic change, see methods) and using this as a surrogate for the unquantifiable spatial variation of the past. We also provide, as an illustrative example of the ways in which this approach could be developed, a brief case study which compares data from our analysis with data gained from pedogenic carbonates from East African hominin localities.

Home ranges

A home range may be defined as a circumscribed area in which an individual spends much of its life, and contains the requisite resources (food, water, shelter and conspecifics to mate with) (Barnard, 1999). This is somewhat different to a territory, which is the section of a home range that is actively defended (Manning and Dawkins, 2012). A territory may cover the entire home range or be restricted to around a particular resource, such as nesting site. Barnard (1999) points out that home range size is not always easy to quantify for extant animals, and it is even harder to infer for extinct taxa. However, there are some general rules than can be applied; for example, home range size (or feeding territory size) tends to be scaled with body mass (Clutton-Brock and Harvey, 1984). This is unsurprising as not only do larger animals require more physical space but they also require more food than smaller animals (McNab, 2012).

Following from these patterns established for extant species, for hominins an increase in range size has been inferred from increasing carnivory (Foley, 2001), a direct result of increasing body size and dietary quality (Leonard and Robertson, 2000, and see below). However, it has proved difficult to gain accurate estimates of home range size, even using modern isotopic techniques (e.g. Copeland et al. 2011), so we have used a variety of measures based on archaeological information and estimates based on data from extant human groups or other animals.

Methods

Calculating landcover

To quantify land cover heterogeneity in a variety of modern African landscapes, we analysed seven Landsat ETM+ satellite image pairs ranging in latitude from Ethiopia to South Africa, and in habitat types from forest to semi-desert (Fig. 1). These were chosen from a larger study of sub-Saharan Africa land cover, in which sites were selected randomly and from these we chose seven sites that we considered representative of the main habitats and geographical locations most often discussed in studies of early human evolution in Africa.

Due to the highly seasonal nature of many African landscapes as a result of climate and rainfall patterns, both wet and dry season Landsat ETM+ satellite imagery was used in combination to generate a single land cover classification for each study area. This enabled land cover classes present, or only able to be discriminated, at certain times of the year, such as seasonal water to be identified. A number of image pre-processing steps were performed on the images using ERDAS IMAGINE 2010 to ensure data quality was maintained. These included: error detection and recording; cloud and cloud shadow masking; image geometric accuracy checking; atmospheric correction; and finally compositing the wet and dry season images into a single dual-date composite image (Morton et al., 2011). For both the wet and dry season Landsat ETM+ images spectral bands 1 (0.45-0.52 μm wavelength), 2 (0.52-0.60 μm), 3 (0.63-0.69 μm), 4 (0.77-0.90 μm), 5 (1.55-1.75 μm) and 7 (2.09-2.35 μm) were used to enable characterisation of the varying wavelength-dependent spectral response of land surface features. Band 6 (thermal, 10.40-12.5 μm) was used only during the cloud masking stage, and was not included in the final composited image. The composite images were projected in the Universal Transverse Mercator (UTM) WGS84 coordinate system.

An unsupervised pixel-based classification technique with post-classification refinement was used to generate land cover maps of the study areas. Unsupervised classification algorithms aggregate all pixels within an image into groupings based on the spectral characteristics of those pixels, with the

clustering process controlled by predetermined parameters for numbers of iterations and classes generated (Loveland and Belward, 1997). Unsupervised classification techniques are well established for land cover mapping applications, and have been used in the production of regional and global land cover maps (Loveland et al., 2000; McGwire et al, 1992; Fleischmann and Walsh, 1991). An unsupervised classification generating 75 spectral classes was produced for the composite image using the Iterative Self-Organising Data Analysis Technique (ISODATA) (Bezdek, 1973). This large number of classes was used to minimise the problem of split land cover class spectral clusters (Horner et al., 1997; Wayman et al., 2001).

High-resolution satellite imagery of the study areas available via public portals such as Google Earth was used as a reference to enable the unsupervised spectral classes to be assigned specific land cover class labels (Loveland et al., 2000; Juang, et al., 2004; Cihlar, 2000) corresponding to the project classification nomenclature in Table 1. Additionally, field surveys conducted in the Kruger National Park, South Africa (shown as area F in Fig. 1), in July 2014 involved further identification of ground truthing locations of known land cover types for validation of the classification generated at this site. This field data was combined with the high resolution imagery-derived validation data and showed good congruence between methodologies (Marston et al. in prep.), however given the logistical challenges of collecting ground truthing data over such broad geographical areas, high resolution reference imagery provided the sole source of validation data for the other sites. The classification nomenclature used was designed to be applied broadly across sub-Saharan Africa and was based on a modified version of the Global Land Cover 2000 Land Cover Map of Africa classification system (Mayaux et al., 2000). Our classification also pays special attention to the forest – grassland gradient, and follows the approach of Torellos-Raventos et al., (2013) which stratified this gradient into five forest to grassland categories at 25% intervals (100-75%, 75-50%, 50-25%, 25-5% and 5-0%). We have amalgamated the latter two categories to form a 25-0% canopy grouping. The generated classification maintained the 30 m spatial resolution of the input Landsat ETM+ imagery.

Although the unsupervised spectral classes generally corresponded well to specific land cover classes, occasionally they contained groups of pixels that when inspected were found to relate to more than one land cover class. For these areas of known misclassification, post-classification refinement in the form of manual knowledge-based enhancement procedures was performed to split these classes into single category sub-classes (Loveland et al., 2000), and also to re-label land cover patches to resolve the spectral confusion between disparate land cover classes.

Multiple unsupervised spectral classes would frequently correspond to the same land cover class in the nomenclature due to the inherent spectral variability of that class. For example, the agriculture

class comprised multiple crop types with different planting, growth cycle, harvesting and watering characteristics which are spectrally distinct when present in the satellite imagery. This enabled the spectral variability of each land cover class to be captured prior to the unsupervised spectral classes being aggregated using well defined merging steps (Juang et al., 2004) until a single merged class for each desired land cover class was achieved.

Accuracy assessment of the classification using ground truth locations was performed. Ground truthing data (i.e. independent verification) of known land cover types was derived from high-resolution imagery of the survey area (e.g. Google Earth), and also from field survey data for site F. The use of higher resolution imagery as a source of validation data for testing the accuracy of classifications derived from coarser resolution satellite products such as Landsat ETM+ imagery is an established technique (Duro et al., 2012; Xie et al., 2008; Cihlar et al., 2003). Due to differences between the Landsat ETM+ and high resolution reference data acquisition dates, all points exhibiting suspected temporal change or human or natural disturbance between the two acquisition dates were disregarded. Classification accuracy assessments are shown in Table 2, and confusion matrices for all study areas are provided as Supplementary Information.

Topographical variability across the buffer extents was also examined using Shuttle Radar Topography Mission (SRTM) digital elevation model (DEM) data. Slope data was derived from the SRTM DEM data, with mean, minimum, maximum and standard deviation variables for both elevation and slope extracted for each buffer using the Geospatial Modelling Environment software. Patch richness for all buffers at each radius size was compared to mean elevation and mean slope data across the dataset (data not shown), and no convincing relationships were found.

Range-size estimates

We have used a number of postulated hominin home range sizes from the literature, deliberately sampling a wide size range, supplemented with estimates based on archaeological and anthropological data. Milton and May (1976) proposed a method of estimating home range sizes for individual primates based on body masses and known group-home range sizes. For group-living primates the range size for an individual was estimated by dividing the group home range size by the numbers of individuals within the group. While this necessarily creates an under-estimate of the area any individual may actually roam, it has been widely used and cited in hominin studies (e.g. Leonard and Robertson, 2000; Antón et al. 2002; Antón and Swisher, 2004). Leonard and Robertson (2000) also included estimates of diet quality (whether ape-like or human-forager-like) to calculate their estimated hominin home range sizes. Their equations were subsequently used in Antón et al.

(2002), but with slightly different results. Here we have used the figures from Antón et al. (2002), taking the smallest estimated hominin range size (38 ha for *Australopithecus africanus* on an ape-like diet) and largest pre-*sapiens* range size (452 ha for *Homo erectus* on a low quality human forager-like diet) (see Table 3). We have also utilised published data on modern Hadza maximum foraging distances (Raichlen et al. 2014). For this home range estimate we used the median distance (~1,100 m) based on the maximum distance travelled during 715 foraging bouts (Raichlen et al., 2014). The largest range size is based on the 13 km distance estimated from the original sources of the raw material found at the Oldowan site of Kanjera, Kenya (Braun et al. 2008). While this estimate is necessarily approximate, it provides a useful larger range size and is one of the few approaches available for estimating range size directly from the archaeological record. We also calculated an intermediate home range size estimate of 2.5 km, covering an area of some 19.6km², as an additional model.

Data cleaning and sample sizes

The calculated home range sizes from Table 3 were overlaid onto the classified images as circular areas (buffers). Circular buffers are the simplest geometric shape with which to undertake these types of analysis. While clearly not capturing the complexity of an animal's daily or yearly movement patterns, they have a long history of use in archaeology as a heuristic device (e.g. Vita-Finzi and Higgs, 1970; Flannery, 1976; Bird et al. 2008, Grove, 2009). Our buffers were fixed on a central point, with increasing radii corresponding to the estimated home range sizes (Fig. 2). There were 300 randomly located central points per image. Once the buffers had been applied around these central points, the data were quality checked to remove all buffers containing any cloud, >80% saltwater or freshwater or >10% anthropogenic land cover classes (arable agriculture, built-up environments, and coniferous plantations). Any point where buffers extended beyond the classified area at any buffer size were also disregarded, and only the central points that remained across all five radii sizes retained for further analysis, ensuring that the same buffers were being examined at each scale. This left a variable number of buffers in the analysis for each study area (area A, n = 19; area B, n = 82; area C, n = 48; area D, n = 31; area E, n = 78; area F, n = 174; area G, n = 164), totalling 596 buffers for each estimated home range size.

Analysis

We calculated patch richness (PR) based on the land cover classifications shown in Table 1. PR is a simple measure of how many land cover types (e.g. open woodland, closed woodland) there are

within each buffer. As we are looking to perform analogous studies of hominin landscapes, for the PR results presented here we removed all land cover types that are clearly anthropogenic, leaving only 'natural' vegetation types present (i.e. if a buffer had a PR of 5, but one of the land cover types was 'built up' we removed it to give a 'natural' PR of 4).

We also calculated the percentage of canopy cover within each randomly placed buffer using four categories. Closed woodland = >75% canopy cover, open woodland = 75% - 50% canopy cover, discontinuous grassland = 50% - 25% canopy cover and continuous grassland = 25% - 0% canopy cover. To make these buffer data directly comparable to the vegetation palaeoproxy data from pedogenic carbonates, where other land covers were present, such as bare or swamp they were disregarded and the four % canopy cover categories were scaled to cover 100% of the buffer.

Transects

Complementary to the randomly located buffers which examine the general PR and land cover variability, targeted higher resolution analysis of the localised areas around rivers was performed. This involved the selection of twenty-one transects in two areas (area B, Kenya, n = 9; area F, South Africa, n=12). Each transect started in and then moved away from a water body or river channel with data extracted every 10 m for 5 km along the transects, with this dense sampling providing highly detailed information on localised landscape variability . Two types of data were extracted for each point along the transect - PR data with the central point of the buffers located on the transect for 4 different buffer sizes (347 m, 1100 m, 1199 m and 2500 m), and the land cover class of each individual transect point. The transect locations were selected by eye to cover areas without human activity (such as tarmac roads, agriculture, etc.). The largest 13 km radii buffer size had the effect of smoothing the PR values to a degree where variability in PR values was lost along the transect extent when sampled at 10 m intervals. Therefore the 13 km radii size was disregarded from this element of the analysis which then focussed on the smaller radii. This did not affect the randomly located sample points due to the greater spacing between them. Note that the transect analyses reported here are intended to be illustrative rather than representative of the full range of possible results.

Results

Accuracy assessment was performed on the land cover classifications for the seven study areas, with high accuracies observed from a minimum of 81.6% (area E) to a maximum of 91.8% (area B) recorded (Table 2). Individual site class error matrices are presented in supplementary information.

Randomly placed buffers

Patch Richness

The results for PR are shown in Table 4. Perhaps unsurprisingly it shows that as the buffer sizes get larger, the number of different habitats within them increases, yet the difference in medians between the smallest and largest buffers are quite modest. The least variation (increase in median PR of 1) is seen in area G (South Africa), and the greatest (increase in median PR of 3) in area D (Rwanda/Burundi) and area F (South Africa/Mozambique).

Table 4 also demonstrates that buffers containing uniform habitats are very rare – only 4 areas have such buffers, and they are mostly present at the smallest size (347 m). So even at the scale of our smallest putative range size habitat mosaics are almost ubiquitous. For area C, 10.42% of the smallest buffers were uniform (n=5), for area B it was 7.32% (n = 6), and areas F and G have two uniform buffers each (1.15% and 1.22% of the sample respectively). In total of the 596 buffers analysed at this smallest size, 2.52% (n=15) were uniform (or non-mosaic) habitats. Of these, at 347 m one was continuous grassland (<25% canopy cover, area G), one was discontinuous grassland (25-50% canopy cover, area F)), seven were closed woodland (>75% canopy cover, area C (n=5), area F (n=1), area G (n=1)), and the remaining six were all semi-desert (area B). For the next largest buffer size, there were only two uniform patches, one of closed woodland in area C and one of semi-desert in area B, while one of closed woodland was still present in area C in the 1199 m buffer.

Percentage of canopy cover

Table 5 shows the median and range values for the closed woodland (>75% canopy cover) within the different buffer sizes. While area A and area G show a >7% increase in median closed canopy cover from the smallest to the largest buffers, there is relatively little variation in medians within the other images and buffer sizes. Continuous grassland (<25% canopy cover) results are shown in Table 6. Overall the continuous grassland category is less common across images (except area C and area G), and again (with the exception of area G) the medians do not differ greatly across buffer sizes. Tables 7 and 8 give the same information for the open woodland (75%-50% canopy cover) and discontinuous grassland (50-25% canopy cover). These also suggest that, with the exception of area G and area A, the median amounts of cover within each category do not change as buffer sizes

increase. In essence, these data are surprisingly scale independent, suggesting that the medians of these land cover types tend not change as the estimated home range sizes get larger.

We also compared the distribution of fraction of wooded canopy cover (%fwc) calculated from pedogenic carbonates from the Nachukui Formation, Koobi Fora (Quinn et al., 2013) with % of canopy cover observed for the central points of our randomly placed buffers in our seven different study areas (Fig. 3). The Nachukui Formation (2.4-1.4Ma) was chosen as a representative dataset for an East African hominin locality, for which the %fwc data had been published (Quinn et al. 2013). The central point from each buffer yielded a result such as '>75% canopy cover' and those that were not on the forest-grassland continuum (i.e. bare, semi-desert, seasonal water and agriculture) were removed from the analysis. The data generated from these central points are directly analogous to those obtained from pedogenic carbonate analyses, as they are both spatially constrained estimates of canopy cover based on an individual point. However, this does not mean that the results of these analyses are analogous. Our examination of areas from Ethiopia to South Africa (Fig. 1) show that there is great variability in land cover at single points within each image (Fig. 3), and that the expected land cover types are found in the appropriate landscapes. For example, 74 out of 82 points are semi-desert or bare in area B (the Turkana region, data not shown), while area F (encompassing the Kruger National Park) shows considerable heterogeneity with the majority of vegetation recorded as discontinuous grassland or open woodland (25-75% canopy cover). Comparison of these canopy cover distributions with the pedogenic carbonate data (Fig. 3) show that none of our modern images with randomly selected buffers has a similar distribution of habitats to that calculated from the pedogenic carbonates, although the pattern in the Nachukui Formation at Koobi Fora is most similar to our results from the southern side of the Rift valley in modern Ethiopia (area A). However, what is striking is the relative lack of closed habitat reconstructed from the pedogenic carbonates. In the Nachukui formation only 1.45% (n=1) of the total sample are reconstructed with >75% canopy, while in all of our study areas bar that of the Turkana region (area B, 0%), closed woodland comprises 14-45% of the central points examined. We also calculated the %fwc for pedogenic carbonates from three key hominin regions (Busidima Formation, Ethiopia, and the Koobi Fora and Olorgesailie Formations, Kenya) using data from Levin (2013). For the 1475 datapoints only 19 (1.3%) represent closed canopy woodland, suggesting considerable under-representation of these environments in the palaeosol datasets.

Transect results

The results of our 21 transects in areas B and F are best viewed as illustrative of the possibilities in modern Africa, rather than the more quantitative random sampling of buffers described above. They were chosen by eye, to allow us to take a 2.5km transect from a channel, without interference from roads, agriculture, etc. We here present results that illustrate the variety seen in these transects, and the resulting potential for these types of analyses.

Patch richness. The greatest patch richness in the majority of transects were found by lakes and rivers, with a decrease in PR as the buffers move away from the water source (Fig. 4a-d). In both area B (Kenya) and area F (South Africa) the changes are seen most abruptly in the smallest estimated hominin home range size (347 m), and vary least with the largest (2500 m). This is expected, as the largest buffer size would still be including the channel and its environs until at least 2510 m away from the water source. Transects in area B have lower numbers of habitats in total (Fig. 4a, b), in comparison with area F (Fig. 4c,d), and there is greater complexity in area F (i.e. PR increases and decreases rather than declining as distance to the water source increases).

Land cover. Our analyses show the land cover at each 10 m point along a 2500 m transect (Fig. 5) in a way that would approximate to a standard field survey, however with remote sensing the transects can be extended for much greater distances than is often feasible in the field. Figure 5 shows two contrasting transects for area B (Turkana). Transect a starts at the edge of Lake Turkana and is largely semi-desert with patches of bare, except for two small patches of open woodland at approximately 2000 m and 2100 m. Transect b starts at the edge of the Turkwel River. The area of semi-desert at the start is an island in the braided channel, and then the main area of riparian woodland is reached and continues for ~620 m, until an abrupt transition to semi-desert and bare patches, with smaller areas of open woodland between 1000-1500 m. The transects for area F (Kruger National Park) show contrasting results (Fig. 5,c,d)– transect c is almost entirely discontinuous grassland, with small patches of continuous grassland and a small area of closed woodland at the channel edge. Transect d begins in seasonal freshwater and is largely open woodland throughout its length, interspersed with small patches of closed woodland. Most notable is that at approximately ~1900 m the transect crosses another stream, which is indicated by the increase in closed woodland at this point. Fig. 5 also shows the calculated %fwc for a fossil pedogenic carbonate transect taken lateral to the river in the Dana Aouli Formation, Ethiopia, dated to ~2.7 Ma (Levin et al., 2004) and converted to our land cover classification. This is a much shorter transect (240 m), but lacks any woodland, suggesting an open area, perhaps more similar to that of transect c without the riparian woodland zone.

Discussion

The spatial resolution of palaeoenvironmental reconstructions seldom, if ever, allow an analysis of the range of resources within a hominin's home range. Here we have developed an alternative complementary approach to such questions in hominin behavioural ecology by using modern African vegetation as an analogue to ask questions about the effect of different putative range sizes on access to resources and the potential effects of water sources on such analyses. We have examined what vegetation types the hominins could access at different home range sizes, and concluded that range size does not greatly affect the number of available habitats at these scales of analysis. Even the smallest (perhaps unrealistic) estimated home ranges have habitat variability similar to the largest. In a palaeoecological context this is an encouraging result as it suggests that the fact that we do not know what the range sizes were for early hominins is not crucial if just considering access to a broad range of vegetation types. However, these results are for randomly placed sampling points and range size does make more of a difference if there is a river present (or absent, see below).

Pedogenic carbonates are our current best method of reconstructing the woody cover of past habitats. However, they may underestimate the densest cover (in part as a result of preferentially forming in more open soils), and are limited to those regions with soils that are appropriate for their formation (Quade and Levin, 2013). While our land cover results are a 1 year snapshot, the carbonates are time-averaged over (possibly) 100s-1000s of years. Thus the pedogenic carbonates give a less complex 'smoother' result with less woody cover than those landscapes that we see in the modern day. We see analysis of satellite imagery as a complimentary method to that of the pedogenic carbonates to examine the potentially 'missing' components within the landscapes. It can be used to match the spatial heterogeneity picked up by fine-scale analysis within individual palaeosols (e.g. at Gona, Quade & Levin (2013)), and allow us to quantify landscape characteristics on continuous regional scales, rather than localised point samples. Remote sensing methodologies can also be used to examine spatial heterogeneity in regions where pedogenic carbonates do not form. While we have not attempted here to directly match modern landscapes to any reconstructed palaeoenvironments, there is clearly the potential to do so. While we cannot match the same vegetation in exactly the same locality as seen in the past, it is likely that a similar mixture of water, grassland and trees can be identified in a number of locations, allowing quantifiable models to be built in future.

Our buffers were randomly located in each image, and the results show that patchy ('mosaic') habitats are very widespread. However, the transect data indicate that the greatest number of habitats (PR) is found near water courses (Fig. 4), and that these are likely to exert an influence for

some distance from the channel (Fig. 5). The habitat variability that water sources introduce are not just the obvious ones of water and riparian woodland, but also for example, seasonal water, swamp, and bare (in gravel bars, etc.). This is important for two reasons – firstly, the highest habitat variability appears to be around water courses, the places that hominins appear to have preferred, but also the places with the appropriate sediments for fossilisation and recovery (see Kullmer, 2007). This has led to suggestions that hominins may not have preferred these habitats, but that we are finding them there as a result of recovery bias (White, 1988). Quinn et al. (2013) demonstrated that lithic sites were significantly more wooded than localities sampled at random within the Koobi Fora and Nachukui formation, and that this association was maintained through the 1.0 Ma time span of deposition. However, the mean woodland density through time was 40 %fwc (Quinn et al. 2013), which in our classification would equate with discontinuous grassland. Either thicker woodland was very rare at the time, in comparison with the present day (Fig. 3), or hominins were seeking these slightly more wooded sites within open areas. Quinn et al. (2013) examine four possible reasons for the association of lithics sites with discontinuous grassland, including the need for shade, access to drinking water, raw materials or specific foodstuffs, and explicitly link them to the presence of water (and by association C3 vegetation, shade and cobbles for tool making). In agreement with Quinn et al. (2013), our results suggest that if hominins preferred areas with high habitat heterogeneity (i.e. ‘mosaic’), then the water courses of Africa are the places to find them, and while we have largely focussed on rivers, the same may also be true of lakes and other water sources (Ashley et al., 2009). This does not rule out the taphonomic explanation but does show that, as mentioned by Roe (1997) and Plummer (2004), there are very many plausible non-taphonomic reasons (beyond just access to drinking water) for utilizing sites near rivers.

Conclusions

Modern African land cover is highly complex, yet at the scales proposed for hominin range sizes, this may be less important than we may have first thought. A key factor driving the variability in habitats appears to be the presence of rivers (or other water bodies), and this result fits with other proxies used to reconstruct hominin palaeoenvironments. Overall, remote-sensing will not and cannot replace these proxies, but it does allow for examination of spatial complexity on a much large scale than is usual, and may also highlight land cover types and patterns of distributions that many have been present but are under-represented in the fossil record.

Acknowledgements

This work was undertaken as part of the *Quantifying the Mosaic* project, funded by the Leverhulme Trust (grant number RPG-2012- 472), and we are very grateful for their support. We also thank Dr Rhonda Quinn (Seton Hall University) for sharing the Nachukui pedogenic carbonate data, Dr Naomi Levin (Johns Hopkins University) for publishing the East African pedogenic carbonate data in an open access format, and Dr Sally Reynolds (University of Bournemouth) for remote sensing data collection and comments on the manuscript. We also thank SANParks and the staff at the Kruger National Park (especially our game guard Kumekani Masinga) for our research permit and facilitating our ground-truthing data collection, and Prof. Paul Aplin (Edge Hill University) for assistance in the field.

References

- Antón, S.C., Leonard, W.R., Robertson, M.L. (2002) An ecomorphological model of the initial hominid dispersal from Africa. *Journal of Human Evolution* 43: 773-785.
- Antón, S.C., Swisher III, C.C. (2004) Early dispersals of *Homo* from Africa. *Annual Review of Anthropology* 33: 271-96.
- Ashley, G.M., Tactikos, J.C., Owen, R.B. (2009) Hominin use of springs and wetlands: Paleoclimate and archaeological records from Olduvai Gorge (~1.79-1.74Ma). *Palaeogeography, Palaeoclimatology, Palaeoecology* 272: 1-16.
- Barnard, C.C. (1999) Home range. In Carlow, P. (ed) *Blackwell's concise encyclopaedia of ecology*. Blackwell Science, Oxford.
- Bezdek, J. C. Fuzzy mathematics in pattern classification, Ph.D. dissertation, Cornell University, Ithaca, New York. 1973.
- Bird RB, Bird DW, Coddling BF, Parker CH, Jones JH. 2008. The 'fire stick farming' hypothesis : Australian Aboriginal foraging strategies, biodiversity, and anthropogenic fire mosaics. *Proc. Nat. Acad. Sci.* 105 : 14796-14801.
- Blome, M.W., Cohen, A.S., Tryon. C.A., Brooks, A.S. (2012) The environmental context for the origins of modern human diversity: A synthesis of regional variability in African climate 150,000-30,000 years ago. *Journal of Human Evolution* 62: 563-592.
- Bowler, P.J. (1986) *Theories of human evolution; a century of debate 1844-1944*. Basil Blackwell, Oxford.

444 Braun, D.R., et al. (2008) Oldowan behavior and raw material transport: perspectives from the
 445 Kanjera Formation. *Journal of Archaeological Science* 35: 2329-2345.

446 Cerling, T.E., Wynn, J.G., Andanje, S.A., Bird, M.I., Kimutai Korir, D., Levin, N.E., Mace, M., Macharia,
 447 A.N., Quade, J., Remien, C.H. (2011) Woody cover and hominin environments in the past 6 million
 448 years. *Nature* 476, 51-56.

449 Cihlar, J. Land cover mapping of large areas from satellites: status and research priorities. *Internat. J.*
 450 *Remote Sens.*, 2000, 21, 1093-1114.

451 Cihlar, J.; Latifovic, R.; Beaubien, J.; Guindon, B.; Palmer, M. Thematic mapper (TM) based accuracy
 452 assessment of a land cover product for Canada derived from SPOT VEGETATION (VGT) data. *Can. J.*
 453 *Remote Sens.* 2003, 29, 154–170.

454 Clutton-Brock, T.H. and Harvey, P.H. (1984) Comparative approaches to investigating adaptation. In
 455 Krebs, J.R. and Davies N.B. (eds) *Behavioural ecology and evolutionary approach*. 2nd ed. Blackwell,
 456 Oxford. Pp 7-29.

457 Copeland, S.R., Sponheimer, M., de Ruiter, D.J., Lee-Thorp, J.A., Codron, D., le Roux, P.J., Grimes, V.,
 458 Richards, M.P. (2011) Strontium isotope evidence for landscape use by early hominins. *Nature* 474:
 459 76-79.

460 Duro, D. C.; Franklin, S. E.; Dube, M. G. Multi-scale object-based image analysis and feature selection
 461 of multi-sensor earth observation imagery using random forests, *Internat. J. Remote Sens.*, 2012, 33,
 462 4502–4526.

463 Flannery, K.V. 1976. Chapter 5: The Village and its catchment area [and sections therein]. In:
 464 Flannery, K.V. (ed) *The early Mesoamerican village*. New York: Academic Press. pp. 91-130.

465 Finlayson, C. (2014) *The improbable primate*. Oxford University Press, Oxford.

466 Fleischmann, C. G.; Walsh, S. J. Multi-temporal AVHRR digital data: an approach for landcover
 467 mapping of heterogeneous landscapes. *Geocarto International*, 1991, 4, 5–20.

468 Foley, R. (2001) The evolutionary consequences of increased carnivory in hominids. Pp. 305-331. In
 469 Stanford, C.B. & Bunn, H.T. (eds) *Meat-eating and human evolution*. Oxford University Press, USA.

470 Grove, M. 2009. Hunter-gatherer movement patterns: causes and constraints. *Journal of*
 471 *anthropological archaeology* 28: 222-233.

472 Habermann, J.M., Stanistreet, I.G., Stollhofen, H., Albert, R.M., Bamford, M.K., Pante, M.C., Njau,
 473 J.K., Masao, F.T. (2016) In situ ~2.0 Ma trees discovered as fossil rooted stumps, lowermost Bed I,
 474 Olduvai Gorge, Tanzania. *Journal of Human Evolution* 90: 74-87.

475 Harmand, S. (2009) Variability in raw material selectivity at the Late Pliocene sites of Lokalalei, West
 476 Turkana, Kenya. In: Hovers, E., Braun, D.R. (eds) *Interdisciplinary approaches to the Oldowan*.
 477 Springer, Dordrecht. pp. 85-97.

478 Homer, C. G.; Ramsey, R. D.; Edwards, T. C. Jr; Falconer, A. Landscape cover- type modeling using a
 479 multi-scene Thematic Mapper mosaic. *Photogramm. Eng. Rem. S.* 1997, 63, 59–67.

480 Juang, H.; Strittholt, J. R.; Frost, P. A.; Slosser, N. C. The classification of seral forest in the Pacific
 481 Northwest USA using Landsat ETM+ imagery. *Remote Sens. Environ.* 2004, 91, 320-331.

482 Kroll, E.M., Isaac, G.LI. (1984) Configurations of artifacts and bones at early Pleistocene sites in East
 483 Africa. In Hietala, H. (ed) *Intrasite spatial analysis in archaeology*. Cambridge University Press,
 484 Cambridge. pp. 4-31.

485 Kullmer, O. (2007) Geological background of early hominid sites in Africa. In: *Handbook of*
 486 *Palaeoanthropology Vol 1: Principles, Methods and Approaches*. Henke, W. & Tattersall, I. (Eds)
 487 Springer, New York. pp. 339-356.

488 Leonard, W.R., Robertson, M.L. (2000) Ecological correlates of home range variation in Primates:
 489 implications for hominid evolution. Pp. 628-648. In: Boinski, S. & Garber, P.A. (eds) *On the move:*
 490 *how and why animals travel in groups*. University of Chicago Press, Chicago.

491 Levin, N.E., Quade, J., Simpson, S.W., Semaw, S., Rogers, M. (2004) Isotopic evidence for Plio-
 492 Pleistocene environmental change at Gona, Ethiopia. *Earth and Planetary Science Letters* 219, 93-
 493 110.

494 Levin, N. E. (2013), *Compilation of East Africa Soil Carbonate Stable Isotope Data*. Integrated Earth
 495 Data Applications (IEDA). doi:10.1594/IEDA/100231

496 Loveland, T. R.; Belward, A. S. The IGBP-DIS global 1km land cover data set, DISCover: first results,
 497 *Internat. J. Remote Sens*, 1997, 18, 3289-3295.

498 Loveland, T. R.; Reed, B. C.; Brown, J. F.; Ohlen, D. O.; Zhu Z.; Yang, L.; Merchant, J. W. Development
 499 of a global land cover characteristics database and IGBP DISCover from 1km AVHRR data. *Internat. J.*
 500 *Remote Sens.*, 2000, 21, 1303-1330.

501 McGwire, K. C.; Fairbanks, D. H. K.; Estes, J. E. Examining regional vegetation associations using
502 multi-temporal AVHRR imagery. Technical Papers of the ASPRS–ACSM Annual Convention,
503 Albuquerque, USA, March 3–5 1992, Vol. 1, pp. 304–313.

504 McNab, B.K. (2012) *Extreme measures; the ecological energetics of birds and mammals*. University of
505 Chicago Press, Chicago.

506 Magill, C.R., Ashley, G.M., Domínguez-Rodrigo, M., Freeman, K.H. (2016) Dietary options and
507 behaviour suggested by plant biomarker evidence in early human habitat. Proceedings of the
508 National Academy of Sciences 113: 2874-2879.

509 Manning, A and Dawkins, M.S. (2012) *An introduction to animal behaviour*. 6th ed. Cambridge
510 University Press, Cambridge.

511 Mayaux, P.; Bartholom, E.; Cabral, A.; Cherlet, M.; Defourny, P.; Di Gregorio, A.; Diallo, O.; Massart,
512 M., Nonguierma, A.; Pekel, J.F.; Pretorius, C.; Vancutsem, C.; Vasconcelos, M. The Land Cover Map
513 for Africa in the Year 2000. GLC2000 database, European Commission Joint Research Centre, 2003.
514 <http://www-gem.jrc.it/glc2000>.

515 Milton, K., May, M.L. (1976) Body weight, diet and home range area in primates. *Nature* 259, 459-
516 462.

517 Morton, D.; Rowland, C.; Wood, C.; Meek, L.; Marston, C.; Smith, G.; Wadsworth, R.; Simpson, I.C.
518 2011. Final Report for LCM2007 - the new UK land cover map. Countryside Survey Technical Report
519 No 11/07 NERC/Centre for Ecology & Hydrology 112pp. (CEH Project Number: C03259).

520 Plummer, T. (2004) Flaked stones and old bones: Biological and cultural evolution at the dawn of
521 technology. *Yearbook of Physical Anthropology* 47: 118-164.

522 Quade, J., Levin, N. (2013) east African hominin palaeoecology: isotopic evidence from palaeosols.
523 In: Sponheimer, M., Lee-Thorp, J.A., Reed, K.E., Ungar, P.S. (eds) *Early hominin palaeoecology*.
524 University Press of Colorado, Boulder.

525 Quinn, R.L., Lepre, C.J., Feibel, C.S., Wright, J.D., Mortlock, R.A., Harmand, S., Brugal, J-P., Roche, H.
526 (2013) Pedogenic carbonate stable isotopic evidence for wooded habitat preference of early
527 Pleistocene tool makers in the Turkana Basin. *Journal of Human Evolution* 65: 65-78.

528 Raichlen, D.A., Wood, B.M., Gordon, A.D., Mbulla, A.Z.P., Marlowe, F.W., Pontzer, H. (2014) Evidence
529 of Levy walk foraging patterns in human hunter-gatherers. *PNAS* 111: 728-733.

530 Roe, D. (1997) Summary and overview. In: Issac, G.Ll. (ed) Koobi Fora research project Volume 5:
531 Plio-Pleistocene archaeology. Clarendon Press: Oxford. Pp. 544-567.

532 Reynolds, S.C., Wilkinson, D.M., Marston, C.G. & O'Regan, H.J. (2015) The "Mosaic habitat" concept
533 in human evolution: Past and present. *Transactions of the Royal Society of South Africa* 70: 57-69.

534 Torello-Raventos, M.,; Feldpausch, T.R.; Veenendaal, E.; Schrod, F.; Saiz, G.; Domingues, T.F.;
535 Djagbletey, G.; Ford, A.; Kemp, J.; Marimon, B.S.; Marimon, Jr B.H.; Lenza, E.; Ratter, J.A.;
536 Maracahipes, L.; Quesada, C.A.; Ishida, F.Y.; Nardoto, G.B.; Affum-Baffoe, K.; Arroyo, L.; Bowman,
537 D.M.J.S.; Compaore, H.; Davies, K.; Diallo, A.,; Fyllas, N.M.; Gilpin, M.; Hein, F.; Johnson, M.; Killeen,
538 T. J.; Metcalfe, D.; Miranda, H.S.; Steininger, M.; Thomson, J.; Sykora, K.; Mougou, E.; Hieraux, P.;
539 Bird, M.I.; Grace, J.; Lewis, S.L.; Phillips, O.L. and Lloyd, J. 2013. On the delineation of tropical
540 vegetation types with an emphasis on forest/savannah transitions. *Plant ecology and diversity*,
541 6:101-137.

542 Vita-Finzi, C., Higgs, E.S. 1970. Prehistoric economy in the Mount Carmel area of Palestine: site
543 catchment analysis. *Proceedings of the Prehistoric Society* 36: 1-37.

544 Wayman, J. P.; Wynne, R. H.; Scrivani, J. A.; Reams, G. A. Landsat TM-based forest area estimation
545 using iterative guided spectral class rejection. *Photogramm. Eng. Rem. S.*, 2001, 67, 1155–1166.

546 White, T.D. (1988) The comparative biology of "robust" *Australopithecus*: clues from context. In:
547 Grine, F.E. (ed.) *The evolutionary history of the "robust" australopithecines*. Aldine: New Brunswick.
548 Pp. 449-484.

549 Xie, Y.; Sha, Z. and Yu, M. Remote sensing imagery in vegetation mapping: a review. *J. Plant Ecol-UK*,
550 2008, 1, 9-23.

551

552 Table 1. Land cover map classification nomenclature.

General habitat	Land cover class and code	Description
Woodland	Closed woodland (CDW)	Closed woodland (75%-100% tree cover)
	Open woodland (ODW)	Open woodland (50%-75% tree cover)
Grassland	Continuous grassland (CG)	Continuous grassland (75%-100% grassland)
	Discontinuous grassland (DG)	Discontinuous grassland (50%-75% grassland)
Anthropogenic classes	Agriculture (AG)	Croplands (>50%) Irrigated croplands Tree crops
	Built-up (BU)	Urban areas and settlements Roads Quarry and open-cast mine
	Closed coniferous woodland (CCW)	Coniferous plantation Felled coniferous plantation
Bare	Bare (BA)	Bare soil
		Bare rock
		Bare gravel (braided rivers)
		Stony desert
		Sandy desert and dunes
		Salt hardpans
		Lava flows
Freshwater	Permanent freshwater (PF)	Permanent waterbodies
	Seasonal Freshwater (SF)	Seasonal waterbodies
	Swamp (SW)	Swamps and wetland areas
Coastal	Saltwater (ST)	Seas and oceans
	Mangrove (M)	Mangrove forests
	Littoral sediment (LS)	Littoral sediment
	Supra-littoral sediment (SLS)	Littoral rock
		Supra-littoral sediment
Semi-desert	Semi-desert (SD)	Supra-littoral rock
		Saltmarsh
Ice and Snow	Ice and Snow (IS)	Semi-desert (bare ground with scattered bushes)
		Permanent ice and snow Seasonal ice and snow
Sodic lake	Sodic lake (SLA)	Sodic lake

553

Table 2. Image locations, acquisition dates and classification accuracies. Note that the timings of dry and wet seasons varied each year, with images selected to best represent the variability in vegetation levels between wet and dry seasons.

Area	Location	Dry season image acquisition data	Wet season image acquisition data	Classification accuracy
A	Ethiopia	7 Mar 2002	24 Apr 2002	82.69%
B	Kenya	15 Oct 2002	5 Feb 2003	91.84%
C	DR Congo / Uganda	9 Jan 2001	25 Nov 2001	86.02%
D	Rwanda / Burundi	17 Aug 2002	13 May 2002	86.89%
E	Malawi / Mozambique	2 Oct 2000	28 Apr 2001	81.64%
F	South Africa / Mozambique	19 Dec 1999	9 Apr 2000	84.73%
G	South Africa	31 July 2001	19 Dec 2000	85.39%

Table 3. The five hominin-relevant buffer sizes used in this study.

Radius (m)	Diameter (m)	Area (ha)	Basis	Reference
347	694	38	<i>A. africanus</i>	Antón et al. (2002)
1100	2200	380	Hadza	Raichlen et al. (2014)
1199	2398	452	<i>H. erectus</i>	Antón et al. (2002)
2500	5000	1963.5		This study
13000	26000	53093	Kanjera	Braun et al. (2008)

Table 4. Median patch richness (and range) results for the 7 study areas at 5 different buffer sizes. PR has been adjusted to remove all anthropogenically-related land covers (agriculture, coniferous plantations and built up areas).

Buffer size (m)	Area A (n=19)	Area B (n=82)	Area C (n=48)	Area D (n=31)	Area E (n=78)	Area F (n=174)	Area G (n=164)
347	4 (2,6)	2 (1,4)	4 (1,6)	4 (3,5)	4 (2,6)	4 (1,6)	4 (1,5)
1100	5 (4,6)	3 (1,5)	5 (1,7)	5 (3,6)	4 (3,7)	5 (3,8)	4 (3,6)
1199	5 (4,6)	3 (2,5)	5 (1,7)	5 (3,6)	4 (3,7)	5 (3,8)	4 (3,6)
2500	5 (4,7)	3 (3,7)	5 (4,7)	6 (4,7)	4 (4,7)	6 (4,8)	5 (4,8)
13000	6 (5,7)	4 (3,7)	6 (5,7)	7 (6,8)	6 (5,7)	7 (6,8)	5 (5,8)

Table 5. Median (and range) of % of closed woodland habitat for the 7 study areas at 5 different buffer sizes (scaled to be 100% across the 4 closed woodland – continuous grassland land cover categories).

Buffer size (m)	Area A (n=19)	Area B (n=82)	Area C (n=48)	Area D (n=31)	Area E (n=78)	Area F (n=174)	Area G (n=164)
347	2.5 (0, 80.5)	0 (0, 100)	16.8 (0, 100)	28.7 (0, 97.0)	42.5 (0, 98.8)	3.9 (0, 100)	7.2 (0, 100)
1100	9.0 (0.3, 59.9)	0 (0, 98.2)	17.2 (0.1, 100)	29.5 (1.6, 88.3)	46.4 (1.9, 94.6)	5.0 (0, 96.4)	10.8 (0, 89.0)
1199	9.4 (0.3, 61.1)	0 (0, 98.8)	17.9 (0.2, 100)	30.0 (1.9, 87.8)	46.3 (2.3, 94.3)	4.9 (0, 96.0)	11.7 (0, 88.4)
2500	6.4 (0.2, 65.0)	0 (0, 77.3)	15.8 (0.5, 99.9)	28.8 (4.7, 78.7)	46.5 (2.2, 91.8)	7.9 (0, 92.3)	15.3 (0, 79.3)
13000	10.2 (1.6, 38.9)	0.3 (0, 52.1)	12.7 (1.1, 99.5)	29.9 (15.1, 45.4)	42.3 (4.7, 86.1)	8.2 (0.6, 66.7)	19.5 (0.3, 47.7)

Table 6. Median (and range) of % continuous grassland habitat for the 7 study areas at 5 different buffer sizes (scaled to be 100% across the 4 closed woodland – continuous grassland land cover categories).

Buffer size (m)	Area A (n=19)	Area B (n=82)	Area C (n=48)	Area D (n=31)	Area E (n=78)	Area F (n=174)	Area G (n=164)
347	1.7 (0, 44.7)	0 (0,0)	36.3 (0, 99.1)	2.9 (0, 41.2)	3.7 (0, 83.0)	3.6 (0, 99.8)	36.5 (0, 100)
1100	3.1 (0, 32.1)	0 (0,0)	38.7 (0, 79.2)	4.4 (0, 29.8)	6.3 (0, 70.2)	4.3 (0, 96.4)	41.7 (2.3, 99.7)
1199	3.4 (0, 30.5)	0 (0,0)	38.7 (0, 80.1)	4.3 (0, 30.2)	7.3 (0, 69.8)	4.6 (0, 96.8)	41.5 (2.2, 99.6)
2500	7.6 (0.4, 35.6)	0 (0, 0.2)	38.3 (0, 77.7)	4.8 (0.6, 25.9)	7.6 (0.1, 67.0)	5.9 (0, 92.6)	42.6 (5.2, 96.1)
13000	9.2 (2.0, 27.7)	0 (0, 2.1)	42.6 (0, 69.4)	5.2 (2.4, 17.3)	8.6 (1.5, 53.6)	8.6 (0.3, 75.1)	45.9 (18.9, 92.4)

Table 7. Median (and range) of % of open woodland habitat for the 7 study areas at 5 different buffer sizes (scaled to be 100% across the 4 closed woodland – continuous grassland land cover categories).

Buffer size (m)	Area A (n=19)	Area B (n=82)	Area C (n=48)	Area D (n=31)	Area E (n=78)	Area F (n=174)	Area G (n=164)
347	3.3 (0, 39.7)	100 (0,100)	2.0 (0, 17.2)	30.8 (1.0, 63.5)	12.9 (0, 56.5)	34.1 (0, 88.8)	6.4 (0, 57.6)
1100	4.1 (0.5, 38.1)	100 (0, 100)	1.8 (0, 7.5)	32.8 (5.0, 61.4)	14.4 (1.7, 57.3)	35.3 (0.2, 74.9)	8.7 (0, 47.9)
1199	4.6 (0.6, 38.0)	100 (0, 100)	1.8 (0, 7.1)	33.5 (5.0, 62.6)	14.6 (1.5, 57.2)	36.0 (0.2, 74.6)	9.0 (0, 46.0)
2500	5.1 (0.5, 29.3)	100 (2.2, 100)	2.2 (0.04, 5.6)	37.0 (9.8, 57.9)	14.2 (2.9, 56.2)	35.2 (0.1, 70.4)	9.9 (0.01, 37.9)
13000	5.7 (2.5, 15.2)	99.7 (37.9, 100)	2.7 (0.2, 4.0)	37.1 (23.9, 43.9)	17.2 (5.5, 42.1)	34.7 (3.4, 55.8)	9.7 (0.6, 23.9)

588 Table 8. Median (and range) of % of discontinuous grassland habitat for the 7 images at 5 different
589 buffer sizes (scaled to be 100% across the 4 closed woodland – continuous grassland land cover
590 categories).

Buffer size (m)	Area A (n=19)	Area B (n=82)	Area C (n=48)	Area D (n=31)	Area E (n=78)	Area F (n=174)	Area G (n=164)
347	76.8 (13.2, 98.8)	0 (0, 63.9)	33.9 (0, 62.5)	28.9 (0, 93.1)	15.2 (0, 77.8)	30.7 (0, 100)	21.0 (0, 73.0)
1100	73.6 (15.3, 98.2)	0 (0, 69.2)	33.4 (0, 58.2)	25.7 (4.6, 67.2)	16.6 (0.6, 69.6)	29.5 (0.4, 96.6)	21.3 (0.3, 66.1)
1199	73.2 (14.3, 98.2)	0 (0, 71.5)	33.3 (0, 57.4)	26.6 (4.6, 66.4)	17.1 (0.6, 70.7)	28.9 (0.4, 96.0)	20.9 (0.4, 65.2)
2500	68.7 (11.9, 95.8)	0 (0, 68.8)	36.5 (0, 52.3)	23.8 (5.2, 63.0)	17.5 (1.6, 70.5)	29.8 (1.7, 92.6)	22.2 (3.5, 57.2)
13000	63.9 (44.9, 82.1)	0 (0, 13.4)	37.2 (0.4, 49.3)	27.6 (14.4, 47.8)	24.6 (5.0, 44.8)	34.7 (6.6, 79.7)	23.7 (6.8, 34.0)

591

592

Figure 1. Location of Landsat ETM+ images used as study areas in this analysis, see Table 2 for details of site locations.

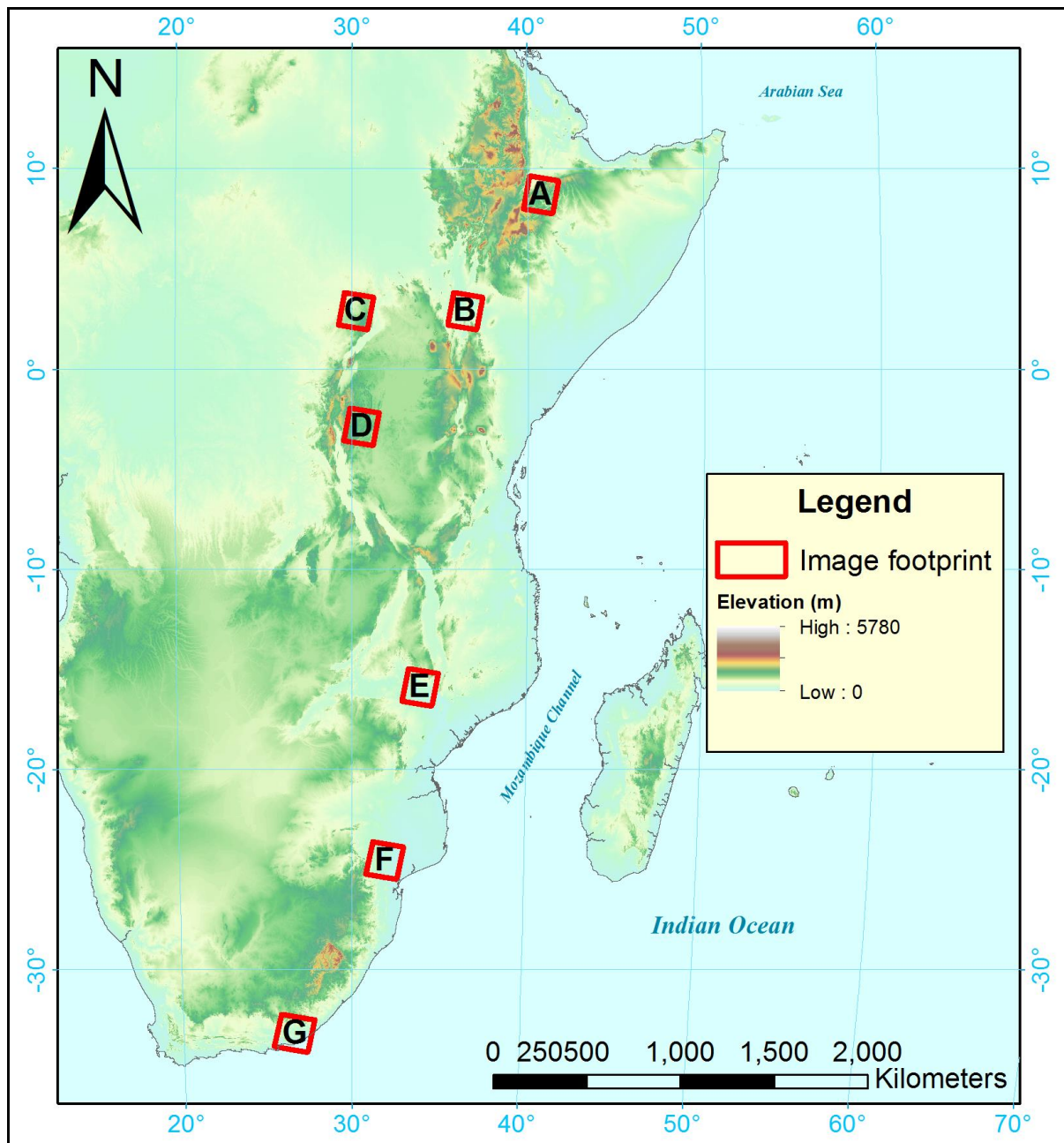


Figure 2. Nested buffers of different radii based on estimated hominin home range sizes, overlaid on land cover classification for area F, the Kruger National Park, demonstrating the land cover variability within different radii.

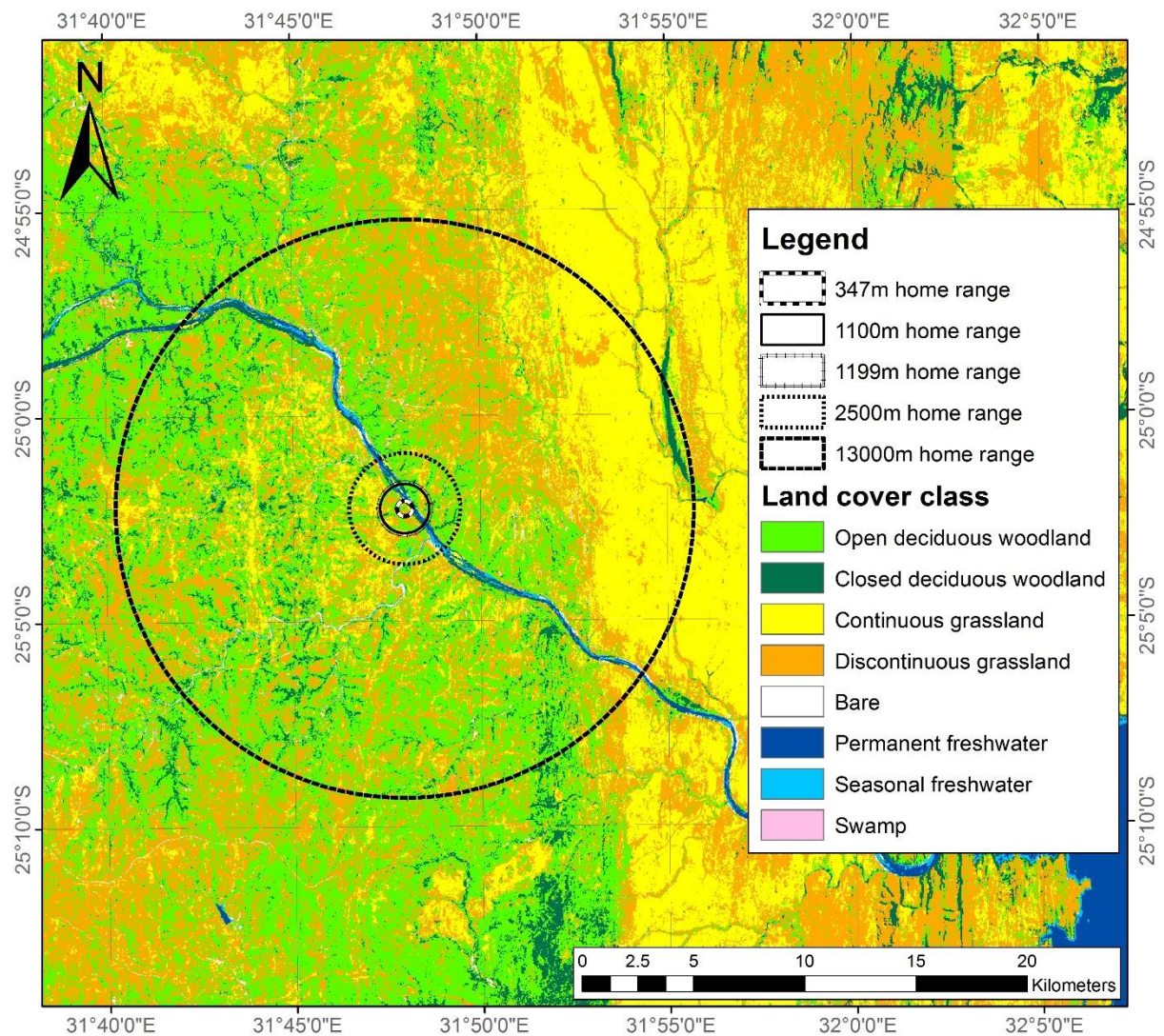


Figure 3. Land cover class frequency for the central points in each randomly placed buffer by study area (A-G) in comparison with % fraction of woody canopy cover (%fwc) from the Nachukui Formation, Koobi Fora calculated from pedogenic carbonates (%fwc methods and data from Quinn et al., 2013). Note: all central points that were not on the forest –grassland continuum (i.e. bare, semi-desert, seasonal water and agriculture) were removed.

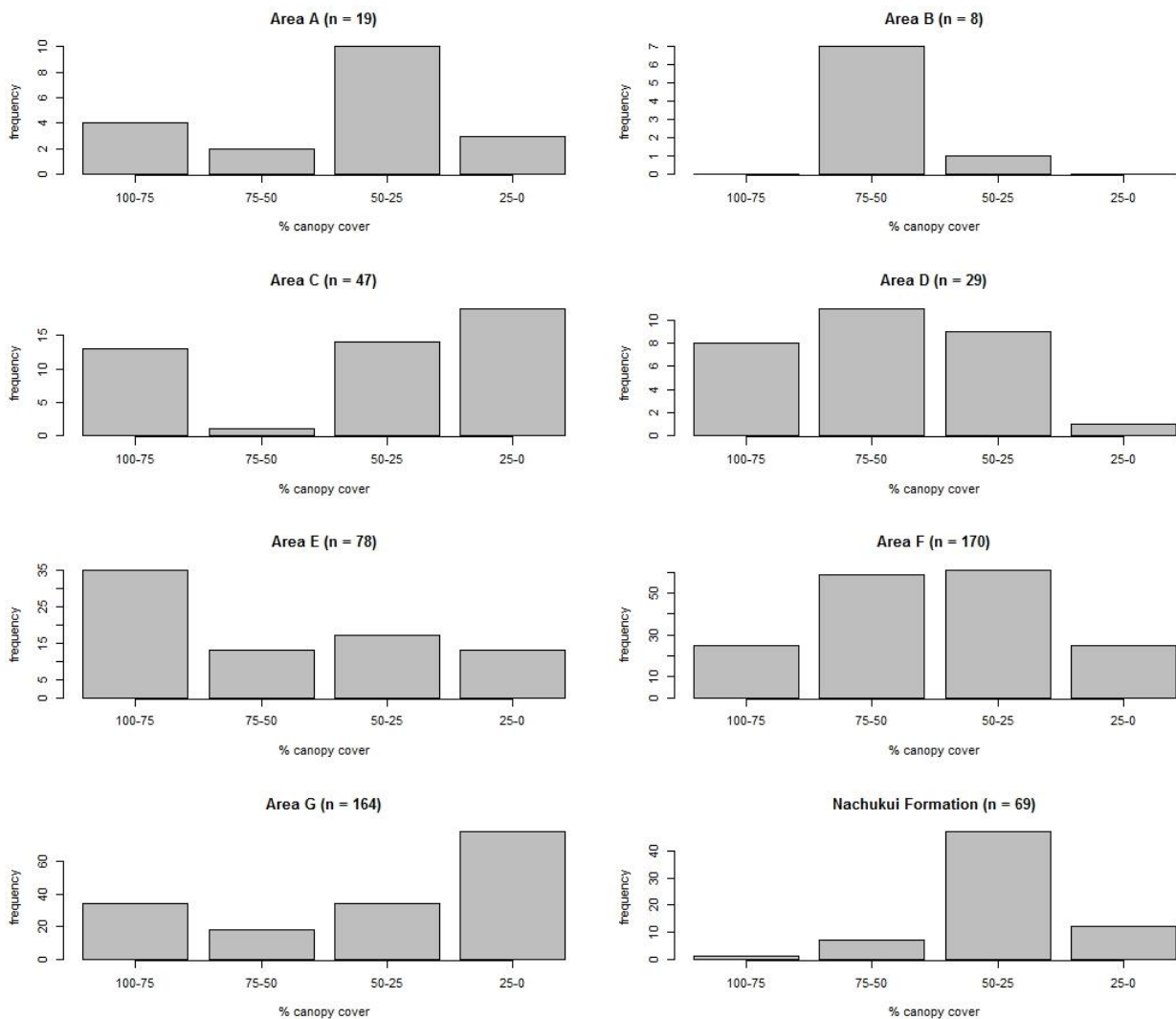
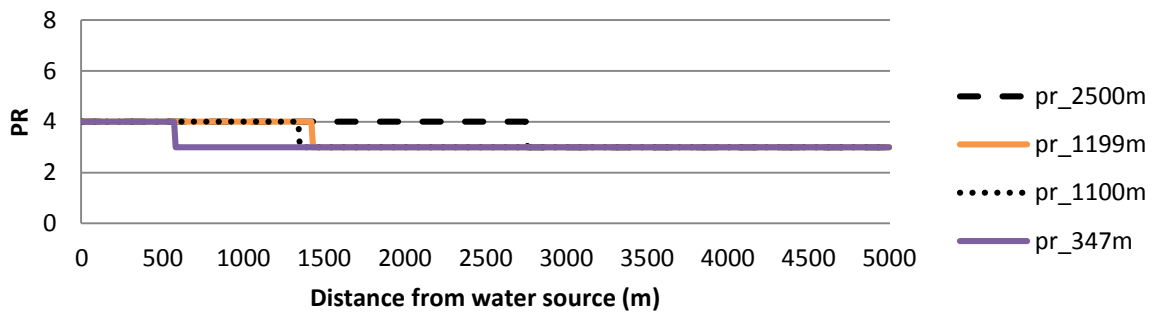
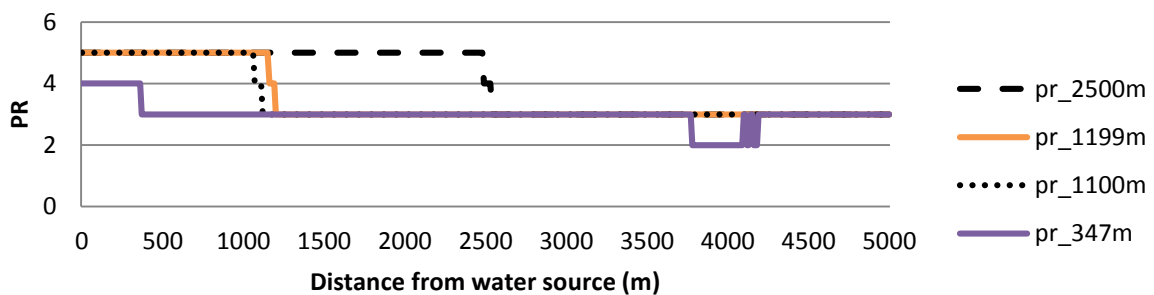


Figure 4. Patch richness over 5000 m transects in Area B (southern Turkana Basin, Kenya) and Area F (Kruger National Park and environs, South Africa). A, b and c illustrate relatively simple transects showing PR largely declining with distance moved away from the water source. a) runs south-west from Lake Turkana, b) runs south-west from the Turkwel River, c) runs southward from the N'wanetzi River, and d) is an example of greater variability in a transect running southward from the N'waswitsontso River.

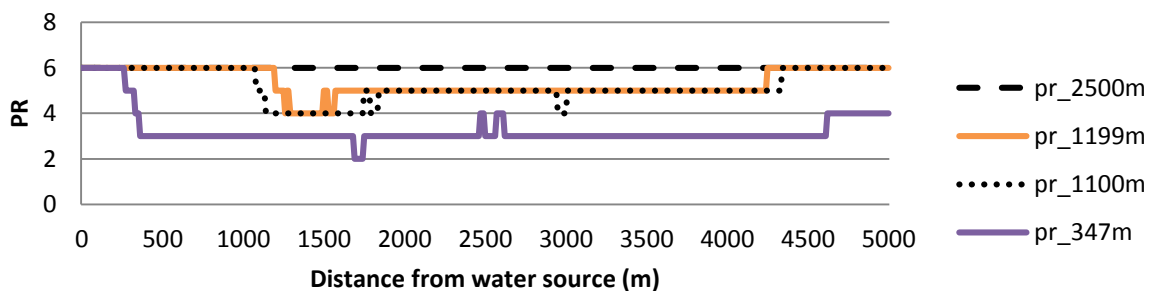
a (Turkana)



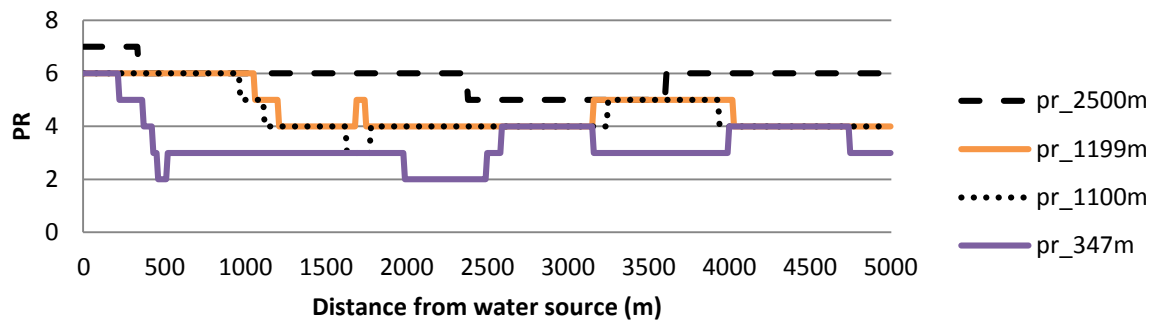
b (Turkana)



c (Kruger)



d (Kruger)



622

623

624

Figure 5. Land cover categories recorded every 10 m for 2500 m starting at a water source, for two transects from Area B (the Turkana region, Kenya), and two from Area F (the Kruger National Park, South Africa). The letters correspond to the PR data shown in Fig. 4 for the same transect locations. Also included for comparison is the fraction of woody cover (f_{wc}) calculated from pedogenic carbonate data from a palaeosol transect from the Dana Aouli Formation, Gona, Ethiopia (Levin et al. 2004), and converted to our land cover classifications.

